Article

Discovery Medicine 2025; 37(200): 1824–1837
https://doi.org/10.24976/Discov.Med.202537200.158

Integrative Transcriptomic Profiling Identifies the GATA3-PRF1 Axis as a Mediator of rTMS-induced Attenuation of Neuropathic Pain After Spinal Cord Injury

Qi Zhu[1], Yibin Zhang[2], Yao Ouyang[3], Yanfei Wu[3], Qian Lv[3], Wei Zhang[3,*]

[1]Department of Respiratory and Critical Care, Zhejiang Provincial People's Hospital, Affiliated People's Hospital, Hangzhou Medical College, 310014 Hangzhou, Zhejiang, China
[2]Department of Respiratory and Critical Care, The Third People's Hospital of Yuhang District, 311115 Hangzhou, Zhejiang, China
[3]Center for Rehabilitation Medicine, Rehabilitation & Sports Medicine Research Institute of Zhejiang Province, Department of Rehabilitation Medicine, Zhejiang Provincial People's Hospital, Affiliated People's Hospital, Hangzhou Medical College, 310014 Hangzhou, Zhejiang, China
*Correspondence: srmyykfkzw@163.com (Wei Zhang)
Submitted: 28 July 2025 Revised: 12 August 2025 Accepted: 19 August 2025 Published: 20 September 2025

Background: Neuropathic pain (NP) following spinal cord injury (SCI) remains a major clinical challenge with limited therapeutic options. This study investigated the mechanism by which repetitive transcranial magnetic stimulation (rTMS) alleviates SCI-induced neuropathic pain (SCI-NP) via the GATA-binding protein 3 (GATA3)-Perforin 1 (PRF1) signaling axis.
Methods: Public transcriptomic datasets (GSE126611, GSE226238, GSE230149) were analyzed to identify candidate rTMS-responsive targets using protein-protein interaction (PPI) and functional enrichment analyses. *In vivo*, a contusive SCI model was induced in male Sprague–Dawley (SD) rats, followed by rTMS treatment (15 Hz, 6 weeks). Pain behaviors were assessed by Hargreaves and von Frey tests. Cytokine expression was quantified by enzyme-linked immunosorbent assay (ELISA), and GATA3/PRF1 expression was measured by Quantitative real-time polymerase chain reaction (qPCR) and Western blot. *In vitro*, binding of GATA3 to the PRF1 promoter was validated in rat spinal neurons using luciferase reporter assays and chromatin immunoprecipitation (ChIP). Functional rescue experiments were performed by intrathecal overexpression of GATA3.
Results: Bioinformatic analyses identified a regulatory interaction between GATA3 and PRF1. rTMS treatment significantly reduced mechanical allodynia and thermal hyperalgesia ($p < 0.05$), downregulated pro-inflammatory cytokines (interleukin (IL)-1β, IL-6, tumor necrosis factor-α (TNF-α); $p < 0.001$), upregulated IL-10 ($p < 0.001$), and suppressed expression of GATA3 and PRF1 ($p < 0.001$). Mechanistically, GATA3 directly bound the PRF1 promoter. GATA3 overexpression abolished rTMS-mediated analgesic and anti-inflammatory effects ($p < 0.05$).
Conclusion: These findings suggest that rTMS alleviates SCI-NP by inhibiting GATA3-mediated transcriptional activation of PRF1, thereby reducing neuroinflammation.

Keywords: repeat transcranial magnetic stimulation; neuropathic pain; spinal cord injury; GATA-binding protein 3; perforin 1

Introduction

Chronic pain following spinal cord injury (SCI) encompasses both musculoskeletal discomfort and neuropathic pain (NP), the latter representing a particularly refractory condition defined as "pain arising from a lesion or disease of the somatosensory nervous system" (International Association for the Study of Pain (IASP) classification) [1,2]. Affecting over 50% of individuals with SCI [3], NP frequently emerges months post-injury and constitutes a primary determinant of long-term disability [4]. Its pathophysiology is multifactorial, including ion channel dysregulation, neuroimmune activation, and disrupted descending modulation, which collectively drive central sensitization [5].

Current treatment strategies remain suboptimal, relying largely on polypharmacy (e.g., antidepressants and antiepileptics) alongside neuromodulation techniques [5]. While spinal cord stimulation has demonstrated clinical utility [6,7], non-invasive alternatives like repetitive transcranial magnetic stimulation (rTMS, $\geq$10 Hz) offer distinct advantages by modulating cortical and subcortical circuits through transcranial magnetic induction [8]. Although rTMS has demonstrated efficacy in depression and other neurological disorders [9–11], its mechanistic actions in SCI-induced NP (SCI-NP) remain unexplored—a critical gap given the unique neuroimmune pathophysiology of this condition.

The GATA transcription factor family, comprising six evolutionarily conserved members (GATA1-6), was ini-

tially characterized by its essential functions in hematopoietic lineages. However, subsequent studies have revealed a broad tissue distribution, with GATA proteins functioning as master regulators of cell type-specific transcriptional programs across multiple biological systems. Among these, GATA-binding protein 3 (GATA3) is canonically recognized for its role in T-lymphocyte differentiation and proliferation [12,13]. Emerging evidence further indicates that GATA3 operates extensively in non-hematopoietic compartments, including the central nervous system, where it modulates neuronal development and survival [14]. Importantly, GATA3 induction have been shown to orchestrate the epigenetic elevation of C-C Motif Chemokine Ligand 21 (CCL21) expression in spinal dorsal horn neurons, thereby mediating bortezomib-evoked NP hypersensitivity [15].

As a core effector protein of the membrane attack complex/perforin (MACPF) family, perforin 1 (PRF1) mediates cytotoxic lymphocyte-mediated target cell lysis through the granule exocytosis pathway in natural killer (NK) cells and cytotoxic T lymphocytes [16]. Beyond its established role in cell-mediated immunity, perforin significantly contributes to immune-mediated disruption of the blood–brain barrier [6]. This highly selective barrier prevents the entry of peripheral immune cells, pathogens, and blood-borne solutes into the central nervous system [17]. However, the association between PRF1 and neurological disorders remains poorly characterized.

Despite emerging evidence implicating neuroinflammation in SCI-NP, the precise immunomodulatory mechanisms underlying non-invasive interventions like rTMS remain elusive. Our integrated bioinformatics analysis revealed a critical protein-protein interaction (PPI) network centered on the GATA3-PRF1 axis, which emerged as a shared molecular signature between SCI-NP pathogenesis and rTMS-responsive genes. Based on these findings, we hypothesized that rTMS alleviates SCI-NP by suppressing GATA3-mediated PRF1 activation, thereby attenuating neuroinflammation. To test this hypothesis, we employed a combinatorial validation spanning behavioral assessments, molecular profiling, and functional genomics in rodent models and neuronal cultures. Our study aims to establish a novel mechanistic link between neuromodulation and adaptive immunity, potentially unveiling new therapeutic targets for refractory NP.

Materials and Methods

Dataset Acquisition

Raw transcriptomic datasets were obtained from the GEO database (https://www.ncbi.nlm.nih.gov/geo/) at the National Center for Biotechnology Information (NCBI). These datasets included GSE126611 (species: *Homo sapiens*), GSE226238 (species: *Homo sapiens*), and GSE230149 (species: *Rattus norvegicus*). GSE126611 included 5 control samples, 4 samples from nerve lesion tissue, and 5 samples with NP. GSE226238 contained RNA sequencing data from whole blood collected from 10 participants with SCI at four time points: within 3 days of injury, 3 months post-injury (MPI), 6 MPI, and 12 MPI, along with 9 healthy controls. GSE230149 included microarray data from 48 rat brains induced by rTMS, consisting of matched sets of hippocampus and parietal cortex samples.

Identification of Differentially Expressed Genes (DEGs)

As described in previous studies [18,19], differentially expressed genes (DEGs) between NP and control groups in GSE126611, as well as between SCI and control groups, were identified using the *limma* and *edgeR* packages. DEGs were filtered by p-value/adjusted p-value < 0.05 and $|\log 2\ (FC)| > 0.3$. Additionally, differential expression analysis of dataset GSE230149, which involved multiple factors (age, cognitive status, and tissue region), was performed. The DEGs identified in the hippocampus were defined as rTMS-associated DEGs (rTMS-DEGs).

Identification and Analysis of Key Genes

The Draw Venn Diagram online tool (https://bioinformatics.psb.ugent.be/webtools/Venn/) was used to establish an intersection for DEGs related to NP and SCI. Pearson correlation analysis was performed within each dataset (SCI and NP), and significantly associated genes were selected ($p < 0.05$). Rat genes were mapped to their human orthologs using the R package *babelgene*. PPI networks were constructed using STRING (https://cn.string-db.org/). Gene Ontology (GO) enrichment analysis—including the cellular component (CC), biological process (BP), and molecular function (MF) categories—was conducted using ClusterProfiler as previously described [20]. Multiple-testing correction was conducted using the Benjamini-Hochberg procedure, and enriched terms with an FDR-adjusted p-value < 0.05 were considered significant.

Establishment of Animal Models

All animal experiments received prior approval from the Laboratory Animal Welfare and Ethics Committee of the Institutional Animal Care and Use Committee, Zhejiang Center of Laboratory Animals (Approval No. ZJCLA-IACUC-20010727), and strictly adhered to the guidelines of the China Council on Animal Care and Use Health. A total of 70 male Sprague–Dawley (SD) rats (8 weeks old, 300–350 g, n = 10/group) were housed under specific-pathogen-free conditions with a 12-h light/dark cycle, temperature maintained at 20–25 °C, and humidity at 45–55%. Anesthesia was induced and maintained using 1% isoflurane. A unilateral SCI was induced at the C5/C6 level of the right hemicord using an Infinite Horizons impactor (Precision Systems and Instrumentation), according to established methods [21]. Precise impact parameters included a

0.7 mm tip diameter, 40 kdynes peak force, and a 2-second dwell period. Sham-operated control animals underwent identical surgical exposure (laminectomy) but did not receive the contusive impact.

rTMS Intervention

rTMS was administered using a MagNeuro device (Magneuro60, VISHEE, Nanjing, China) equipped with a figure-8 coil (outer wing diameter: 100 mm). Intervention commenced 48 h post-surgery. To optimize stimulus delivery and minimize potential artifacts, animals (n = 10) were placed in polypropylene restrainers within a controlled environment free of external electromagnetic interference. Using a stereotaxic frame, the animals' heads were precisely positioned beneath the coil center. The resting motor threshold (RMT), operationally defined as the minimal single-pulse TMS intensity required to evoke a visible hindlimb muscle twitch, was determined empirically for each subject. Subsequent treatment sessions utilized 80% of this individually determined RMT value as the stimulus intensity, which typically corresponded to approximately 40% of the device's maximal output. Each subject received high-frequency rTMS (HF-rTMS) daily, comprising 2400 pulses delivered using the following parameters: frequency, 15 Hz; train duration, 10 pulses; inter-train interval, 20 s; 20 trains per session; administered once daily, 6 days per week, for 6 weeks. Rats assigned to the Sham (n = 10) and Mod (n = 10) groups underwent identical placement procedures, but the coil was oriented perpendicularly (90°) to the cranial surface, ensuring auditory exposure without effective cortical stimulation. Most procedures were based on previous research [22].

Grouping and Treatment

In the first part, SD rats were randomly assigned to three experimental groups under blinded assessment: (1) Sham group: underwent laminectomy at T10 without spinal impact injury; (2) Mod group: SD rats received unilateral contusion injury followed by no intervention; (3) Mod + TMS group: SD rats received unilateral contusion injury followed by TMS.

In the second part, SD rats were randomly assigned to four experimental groups under blinded assessment: (1) Mod group: SD rats received unilateral contusion injury followed by no intervention; (2) Mod + TMS group: SD rats received unilateral contusion injury followed by TMS; (3) Mod + TMS + NC group: SD rats received unilateral contusion injury followed by rTMS and negative control plasmids were administered intrathecally; and (4) Mod + TMS + GATA3 group: SD rats received unilateral contusion injury, followed by rTMS and GATA3-overexpressing plasmids administered intrathecally. At the end of the experiment, all animals were sacrificed by an intraperitoneal injection of 2% pentobarbital sodium (100 mg/kg). Immediately after death, the rats were fixed in the supine position on an anatomical plate. The dorsal skin was disinfected with 75% ethanol, and spinal cord tissue samples were collected.

Thermal Sensory Testing

Thermal nociceptive thresholds were quantified using the Hargreaves apparatus (Ugo Basile, Varese, Italy) according to established protocols. Animals were acclimated to the testing environment for 5 consecutive days (1 h/day) prior to baseline measurements. Preoperative baselines were collected one week before surgery, and postoperative assessments were conducted weekly for six weeks. During testing, animals were manually restrained on a temperature-controlled glass platform, with an infrared emitter precisely positioned beneath the targeted hindpaw. Following stimulus initiation, paw withdrawal latency (PWL) was measured. The radiant heat intensity remained constant across all subjects and sessions. The stimulus intensity yielded a mean baseline PWL of 20 sec, consistent with prior studies utilizing the same unilateral cervical contusion model and testing parameters [21]. Paw mobility remained unrestricted, and withdrawal was defined as a rapid reflex away from the stimulus source, frequently accompanied by licking. Each paw underwent three sequential trials per testing session, administered in alternated order with 120-sec intertrial intervals.

Tactile Sensory Assessment

Mechanical sensitivity was evaluated using the von Frey filament assay, performed previously described [21]. Animals were habituated for 5 days (1 h/day) in plexiglass enclosures positioned on an elevated wire mesh grid, which allowed free movement. Calibrated Semmes-Weinstein monofilaments (Stoetling Co., Kiel, WI, USA; force range: 0.07–2.0 g) were applied perpendicularly to the plantar surface of the hindpaw, avoiding the footpads. The "up-down" method was employed, with each filament applied ten times per paw. The withdrawal threshold was calculated as the filament eliciting a positive response in $\geq$50% of applications, requiring a minimum of three valid stimulations. Assessments were performed one week pre-surgery and continued weekly for six weeks postoperatively.

Cytokine Quantification

Spinal cord tissue homogenates were prepared in RIPA lysis buffer (R0010, Solarbio, Beijing, China) containing Protease Inhibitor Cocktail Set IV (539136, Solarbio, Beijing, China). Following centrifugation at 12,000 $\times$g for 20 min at 4 °C, the resulting supernatants were collected. Concentrations of interleukin-1β (IL-1β, RLB00), interleukin-6 (IL-6, R6000B), tumor necrosis factor-α (TNF-α, DY510), and interleukin-10 (IL-10, DY522) were determined using commercially available enzyme-linked immunosorbent assay (ELISA) kits specific for rat cytokines (R&D Systems, Minneapolis, MN, USA), strictly

adhering to the manufacturer's recommended protocols. Absorbance measurements were performed at a wavelength of 450 nm utilizing a microplate reader.

Quantitative Real-time Polymerase Chain Reaction (qPCR)

Total RNA was isolated from cells or tissue samples using the TRIzol™ Plus RNA Purification Kit (12183555, Thermo Fisher Scientific, Waltham, MA, USA). Purified RNA underwent reverse transcription into complementary DNA (cDNA) using the SuperScript™ VILO™ cDNA Synthesis Kit (Thermo Fisher Scientific, 11754050, Waltham, MA, USA). qPCR amplification was performed using the resultant cDNA, gene-specific primers (listed below), and Fast SYBR™ Green Master Mix (Thermo Fisher Scientific, 4385612, Waltham, MA, USA) on a QuantStudio™ 7 Pro Real-Time PCR System (Thermo Fisher Scientific, A43165, Waltham, MA, USA). *GAPDH* served as the endogenous reference control for normalization. Relative transcript levels for target genes were calculated using the $2^{-\Delta\Delta Ct}$ method.

Primers:

GATA3-F: 5′-CTGCAATGCCTGTGGGCTGTA-3′

GATA3-R: 5′-GTGGCTGGAGTGGCTGAACG-3′

PRF1-F: 5′-CGGCTCACACTGCCAGCGTAATGT-3′

PRF1-R: 5′-CCATCCAGGGTCAGCTGACAGGTA-3′

GAPDH-F: 5′-CCGCATCTTCTTGTGCAGTG-3′

GAPDH-R: 5′-ACCAGCTTCCCATTCTCAGC-3′

Western Blotting (WB)

Cellular and tissue lysates were prepared in ice-cold RIPA lysis buffer containing Protease Inhibitor Cocktail Set IV. Protein concentrations were determined using a bicinchoninic acid (BCA) assay kit (PC0020, Solarbio, , Beijing, China). Equal amounts of protein from whole lysates or isolated RNA-binding protein complexes were resolved by sodium dodecyl sulfate-polyacrylamide gel electrophoresis (SDS-PAGE) and transferred onto polyvinylidene fluoride (PVDF) membranes. Membranes were blocked for 1 h at room temperature using a commercial blocking buffer (37581, Thermo Fisher Scientific, Waltham, MA, USA). Primary antibody incubations were performed overnight at 4 °C, followed by 1-h incubation with horseradish peroxidase (HRP)-conjugated secondary antibodies at room temperature. Protein bands were detected using BeyoECL Plus chemiluminescent substrate (P0018S, Beyotime, Shanghai, China) and visualized utilizing an iBright CL750 imaging system (Thermo Fisher Scientific, Waltham, MA, USA). Densitometry analysis was performed using the integrated iBright software. GAPDH immunoblotting served as the loading control for data normalization.

Antibodies from Abcam (Cambridge, UK) were listed: GATA3 (ab282110, 1:1000, 48 kDa), PRF1 (ab256453, 1:1000, 61 kDa), and GAPDH (ab8245, 1:1000, 36 kDa); Secondary antibodies: anti-rabbit IgG (ab175781, 1:10,000) or anti-mouse IgG (ab205719, 1:2000).

Cell Culture

Rat spinal cord neurons (CP-R144, Procell, Wuhan, China) were cultured in DMEM (SNM-003B, sunncell, Wuhan, China) containing 10% fetal bovine serum (FBS, AW-FBS-001, AnWei-sci, Shanghai, China) and 1% Penicillin-Streptomycin (V900929, Sigma-Aldrich, St. Louis, MO, USA). All cells had undergone cell line authentication and were incubated at 37 °C and 5% CO_2. All cell lines were validated by morphological identification and tested negative for mycoplasma.

Luciferase Assay

The putative GATA3-binding site within the PRF1 promoter region was cloned into the pGL3-Basic vector (Promega, Madison, WI, USA), generating the wild-type reporter construct (pGL3-PRF1-promoter). A corresponding mutant reporter construct (pGL3-PRF1-mut) was engineered by introducing specific nucleotide substitutions into this predicted binding motif using site-directed mutagenesis. Rat spinal cord neurons were co-transfected with the relevant pGL3 reporter plasmid (either wild-type or mutant) and a GATA3-overexpressing plasmid. Following a 48-h incubation period post-transfection, firefly and Renilla luciferase activities were quantified sequentially using the Dual-Luciferase® Reporter Assay System (E1910, Promega, Madison, WI, USA) according to the manufacturer's protocol. Firefly luciferase activity, representing PRF1 promoter activity, was normalized to the co-transfected Renilla luciferase activity as an internal control for transfection efficiency. Relative luciferase activity (RLA) was calculated as the ratio of firefly/Renilla luminescence for each sample.

Chromatin Immunoprecipitation (ChIP)

Chromatin immunoprecipitation (ChIP) assays were performed using the Magna ChIP™ Kit (17-10085, Sigma-Aldrich, St. Louis, MO, USA) according to the manufacturer's protocol with modifications. Briefly, protein-DNA complexes in cultured cells were cross-linked with 1% formaldehyde for 10 min at room temperature, and the reaction was quenched with 0.125 M glycine. Chromatin was subsequently fragmented by sonication using a Bioruptor® system (Diagenode) to generate DNA fragments of 200–500 bp. Immunoprecipitation was carried out overnight at 4 °C with either 5 µg of anti-GATA3 antibody (ab199428, Abcam, Cambridge, UK) or equivalent amounts of species-matched IgG control antibody (ab207997, Abcam, Cambridge, UK). Antibody-chromatin complexes were captured with protein A/G magnetic beads (ab286842, Abcam, Cambridge, UK) for 2 h. Beads were sequentially washed with low-salt, high-salt, and LiCl buffers. Bound com-

plexes were eluted in freshly prepared elution buffer (1% SDS, 0.1 M $NaHCO_3$), and cross-links were reversed by incubating with 200 mM NaCl at 65 °C overnight. DNA was purified and analyzed by qPCR using primers specifically targeting the promoter region of the *PRF1* gene (forward: 5′-CTGTTTAGATTCTCGACTCT-3′; reverse: 5′-GTAGGGAGAGATACTCAAAG-3′). Relative enrichment of target genomic loci was calculated as percentage input after normalization to IgG controls.

Intrathecal Injection

The GATA3 overexpression plasmid (Yunzhou Biosciences Co., Ltd., Guangzhou, China) was incubated with *in vivo*-jetPEI (101000040, Polyplus, Strasbourg, France) for 15 min to form a transfusion complex, which was administered intrathecally into 10 rats according to established protocols [23]. Animals were anesthetized with sodium pentobarbital anesthesia (50 mg kg^{-1}, intraperitoneal injection), and a laminectomy was performed at the L5 vertebra. An 8 G needle was used to puncture the dura mater, after which a polyethylene-10 catheter was inserted into the L4–L6 subarachnoid space via the L5/L6 intervertebral space. The catheter tip was positioned adjacent to the L4–L6 spinal segments. Post-implantation, animals recovered for 5 days prior to experimentation. Rats that developed hindlimb neurological deficits (paresis or paralysis) were excluded. Negative control plasmids were administered intrathecally in an additional group of 10 rats.

Statistical Analysis

Continuous data are presented as mean ± standard deviation (SD). For comparisons among more than two groups, one-way analysis of variance (ANOVA) or two-way ANOVA (Fig. 4A–D, Fig. 6E–H) was applied, followed by Tukey's post hoc test when overall significance was detected. Differences between two experimental groups were assessed using Student's *t*-test. A p-value < 0.05 was defined as statistically significant. All analyses were conducted using GraphPad Prism software (version 9.0, GraphPad Software, San Diego, CA, USA). Behavioral assessment and histological analysis were performed by investigators blinded to conditions.

Results

Bioinformatics Analysis Identified Potential Targets of TMS in SCI-NP

A total of 3508 DEGs were discovered between SCI and control samples in dataset GSE226238 (Fig. 1A). In parallel, 263 DEGs were detected between NP and control samples in dataset GSE126611 (Fig. 1B). The intersection of these datasets revealed 34 common DEGs (coDEGs; Fig. 1C). Pearson correlation analysis of the coDEGs within both SCI and NP datasets (sig-coDegs) demonstrated that all 34 coDEGs were included in this correlated set, with each gene significantly correlated with at least one other gene (Fig. 1D,E).

Analysis of dataset GSE230149 showed DEGs between rTMS and control groups in the hippocampus and parietal cortex after adjusting for age and cognitive status. As exhibited in Fig. 2A, 474 DEGs were identified in the hippocampus. After merging and removing duplicates, 465 unique rTMS-DEGs were obtained. Of these, 169 rTMS-DEGs could be mapped into the human genome (Fig. 2B). To elucidate potential therapeutic targets of rTMS in SCI-NP, we performed correlation analyses between the 169 rTMS-DEGs and the 34 sigcoDegs identified from GSE226238 and GSE126611 datasets. SigCoDEGs represent the intersection of SCI- and NP-associated DEGs, totaling 34 genes. In the SCI dataset, rTMS-DEGs shared 29 co-expressed genes with the sigCoDEGs, all of which mapped to human genes. In the NP dataset, 74 co-expressed genes were identified, 68 of which aligned with human genes. Intersection analysis, therefore, revealed 29 significant related (with 34 sigcoDegs) genes among 169 rTMS-DEGs in the SCI dataset (GSE226238) and 68 in the NP dataset (GSE126611). After merging and removing duplicates, 103 unique candidate targets were identified for further investigation (Fig. 2C).

The PPI network diagram is presented in Fig. 3A, which indicates that GATA3 and PRF1 were strongly correlated genes among the 103 candidate targets. The results of the GO analysis were primarily associated with immune cells (lymphocytes, leukocytes, B cells, and T cells), reflecting their involvement in immune responses (Fig. 3B). Moreover, Fig. 3B highlights GO terms closely related to the mechanisms of rTMS, SCI, and NP, with a large number of genes enriched in lymphocyte differentiation and regulation of leukocyte differentiation.

rTMS Treatment Significantly Improved Behavioral and Inflammatory Phenotypes in the SCI-NP Model

Compared with the sham group, rats in the model (Mod) group developed significant thermal hyperalgesia and mechanical allodynia in the ipsilateral forepaw (Hargreaves test: $p < 0.01$; von Frey test: $p < 0.001$; Fig. 4A,B). rTMS treatment markedly attenuated these nociceptive hypersensitivities in model rats (ipsilateral forepaw: Hargreaves $p < 0.01$, von Frey $p < 0.001$; Fig. 4A,B). A consistent pattern of analgesia was observed in the contralateral forepaw, where rTMS reversed both thermal hyperalgesia (Hargreaves test: $p < 0.05$) and mechanical allodynia (von Frey test: $p < 0.01$) induced by SCI (Fig. 4C,D). These findings indicate that rTMS effectively improved the behavioral phenotypes of the SCI-NP model.

ELISA analysis further revealed significant dysregulation of spinal cytokine profiles in SCI-NP rats. Compared to sham-operated controls, model animals exhibited markedly elevated concentrations of pro-inflammatory me-

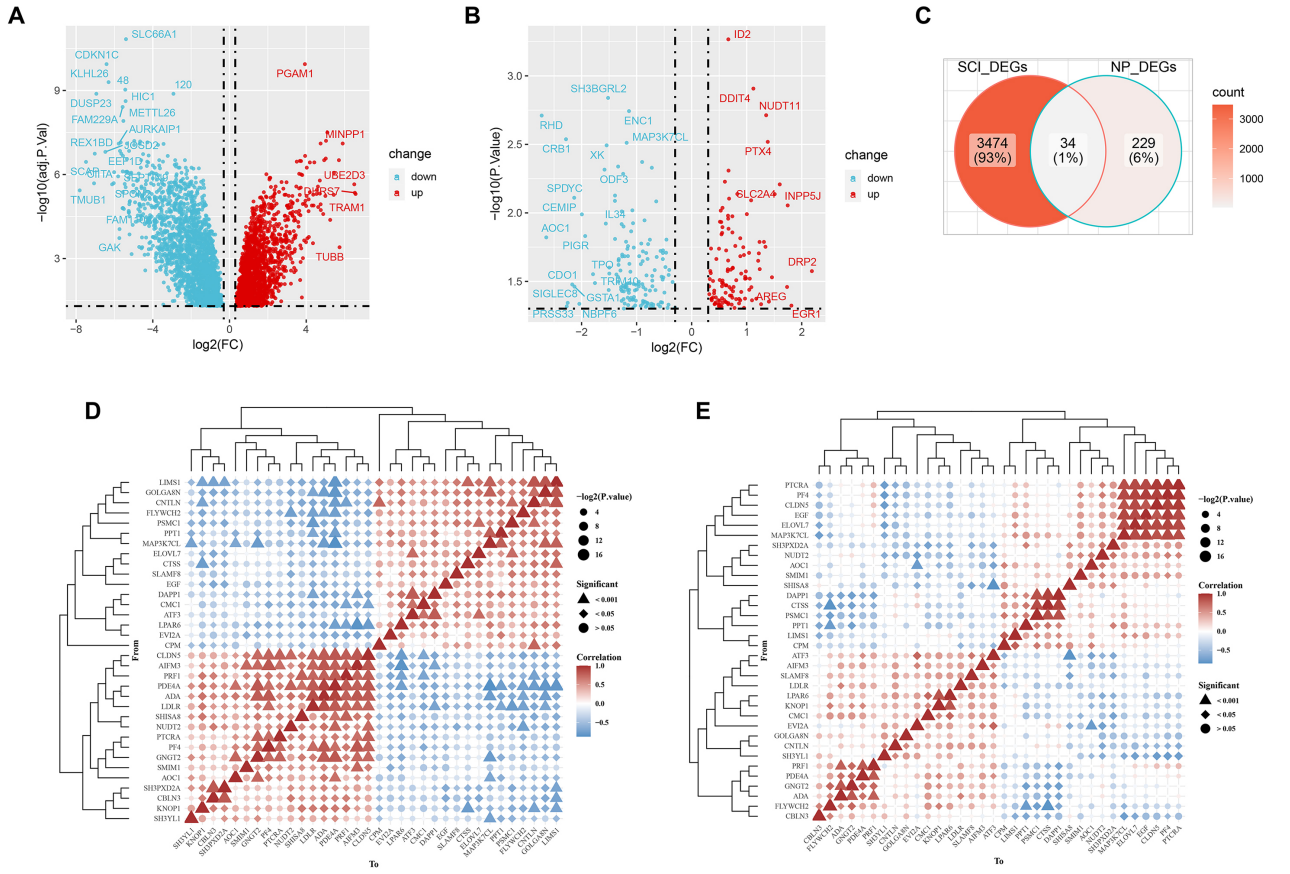

Fig. 1. DEGs in SCI and NP datasets and their intersection. (A) Volcano plot of DEGs between SCI and control samples in dataset GSE226238. (B) Volcano plot of DEGs between NP and control samples in dataset GSE126611. (C) Venn diagram of DEGs related to SCI and NP. (D) Heatmap of correlation analysis for coDEGs and their data in SCI dataset. (E) Heatmap of correlation analysis for coDEGs and their data in NP dataset. DEGs, differentially expressed genes; SCI, spinal cord injury; NP, neuropathic pain; coDEGs, common DEGs.

diators IL-1β, IL-6, and TNF-α (Fig. 4E–G; $p < 0.001$), accompanied by a marked reduction in the anti-inflammatory cytokine IL-10 levels in the injury cohort (Fig. 4H; $p < 0.001$). rTMS intervention effectively normalized these pathological alterations, suppressing IL-1β, IL-6, and TNF-α overexpression (Fig. 4E–G; $p < 0.001$), while restoring IL-10 production (Fig. 4H; $p < 0.001$), thereby re-establishing neuroimmune homeostasis.

Concomitant molecular analysis demonstrated rTMS-mediated suppression of the GATA3-PRF1 axis. Quantitative PCR and immunoblotting demonstrated coordinated upregulation of GATA3 and PRF1 transcripts and proteins in the spinal cords of untreated SCI-NP models (Fig. 4I–M; $p < 0.001$). Importantly, rTMS administration significantly downregulated both targets ($p < 0.001$ *vs* model group), establishing their responsivity to neuromodulation (Fig. 4I–M).

rTMS Exerts Protective Effects in the SCI-NP Model Through Inhibition of the GATA3-PRF1 Axis

To investigate the mechanistic role of the GATA3-PRF1 axis in rTMS intervention for SCI-NP, CP-R144 cells were transfected with GATA3 overexpression plasmids. Compared to the negative control (NC) group, GATA3 overexpression significantly increased both mRNA and protein levels of GATA3 and PRF1 (Fig. 5A–E; $p < 0.001$). Bioinformatic prediction using JASPAR identified a binding motif for GATA3 within the PRF1 promoter region (Fig. 5F). This interaction was functionally validated using a dual-luciferase reporter assay, demonstrating enhanced transcriptional activity upon GATA3 binding (Fig. 5G; $p < 0.001$). In addition, ChIP assays further confirmed direct binding of GATA3 to the PRF1 promoter *in vitro* (Fig. 5H; $p < 0.001$). Collectively, these findings establish that GATA3 transcriptionally activates PRF1 expression.

In vivo, intrathecal overexpression of GATA3 in rTMS-treated SCI-NP models effectively reversed the transcriptional repression induced by magnetic stimulation. Both mRNA and protein expression of GATA3

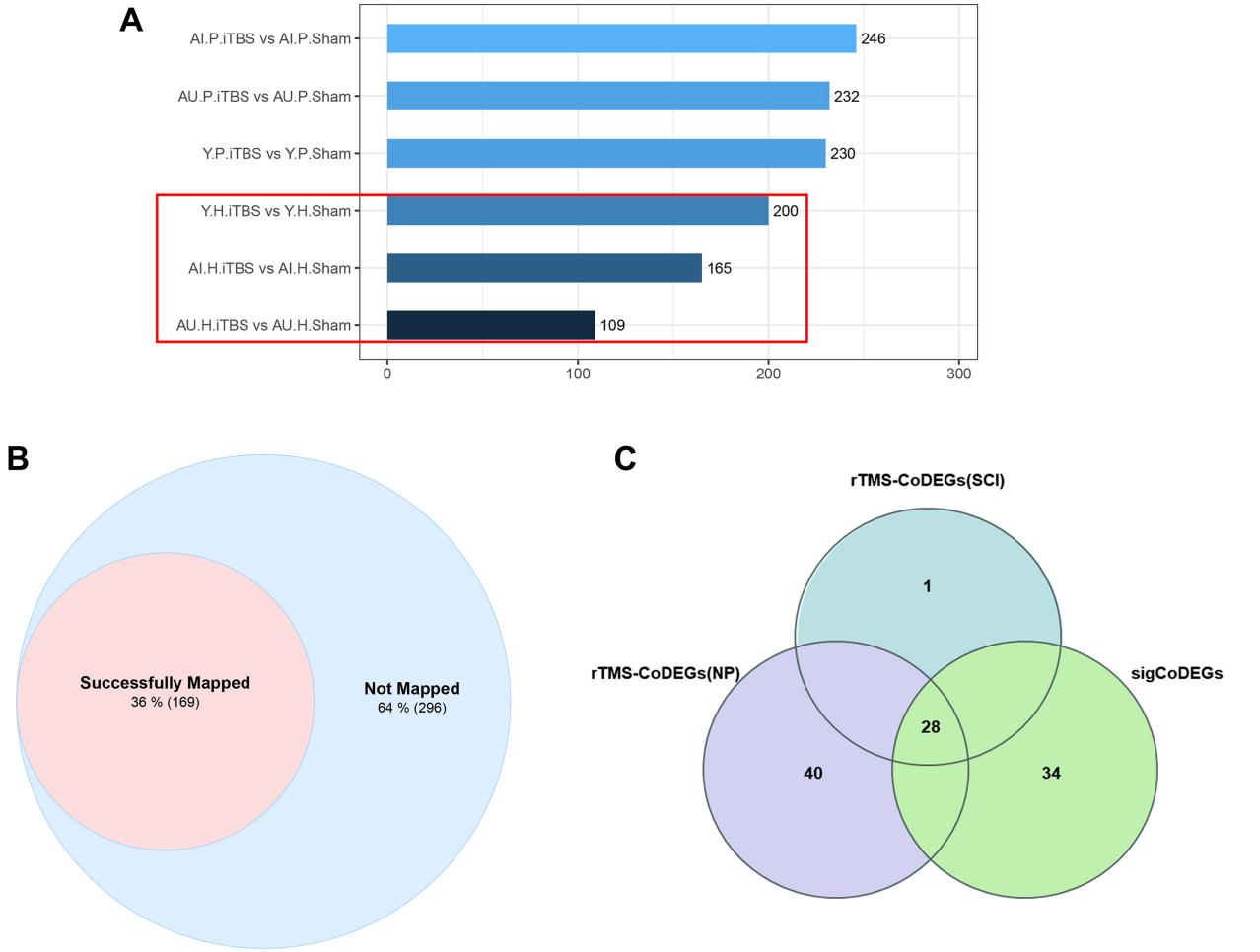

Fig. 2. rTMS-related DEGs in SCI-NP. (A) Bar chart of DEGs between rTMS-treated and sham samples of hippocampus and parietal cortex tissues in Y, AI, and AU rats. 474 DEGs were identified in the hippocampus (highlighted by red box). (B) Venn diagram mapping from rat genes to human genes. (C) Related genes with coDEGs among rTMS-DEGs in GSE226238 and GSE126611 datasets. rTMS, repeat transcranial magnetic stimulation; iTBS, intermittent theta-burst stimulation; Y, Young; A, Aged; I, Impaired; U, Unimpaired; H, Hippocampus; P, Parietal cortex; sigCoDEGs, common DEGs-related in SCI and NP datasets.

and its downstream effector PRF1, which were significantly suppressed by rTMS ($p < 0.01$), exhibited significant restoration upon GATA3 delivery (Fig. 5I–M; $p < 0.001$). Consequently, this genetic intervention triggered pro-inflammatory rebound, characterized by elevated IL-1β, IL-6, and TNF-α concomitant with reduced IL-10 in spinal cord tissues ($p < 0.001$ *vs* Mod + rTMS + NC group; Fig. 6A–D). Consistently, behavioral analyses further confirmed functional reversal, where the analgesic effects of rTMS on bilateral forepaw thermal hyperalgesia and mechanical allodynia were abolished (Fig. 6E–H; $p < 0.05$). These rescue experiments demonstrate that transcriptional inhibition of the GATA3-PRF1 signaling pathway constitutes the primary mechanism by which rTMS alleviates the neuropathic sequelae of SCI.

Discussion

This study demonstrates that rTMS alleviates SCI-NP through a novel immunomodulatory mechanism, specifically by inhibiting GATA3-dependent transcriptional activation of PRF1 in cytotoxic immune cells, thereby attenuating neuroinflammatory cascades.

Emerging evidence suggests that neuroimmune dysregulation contributes to SCI-NP; however, the transcriptional mechanisms underlying neuromodulatory interventions remain poorly defined. Through integrated bioinformatic and experimental analysis, we identified the GATA3-PRF1 axis as a critical pathway linking rTMS to immune regulation. Bioinformatic intersection of SCI/NP-associated genes with rTMS-responsive targets highlighted GATA3 and PRF1 as central regulators. Functional validation demonstrated that GATA3 directly binds to the PRF1 promoter, as shown by luciferase reporter and ChIP as-

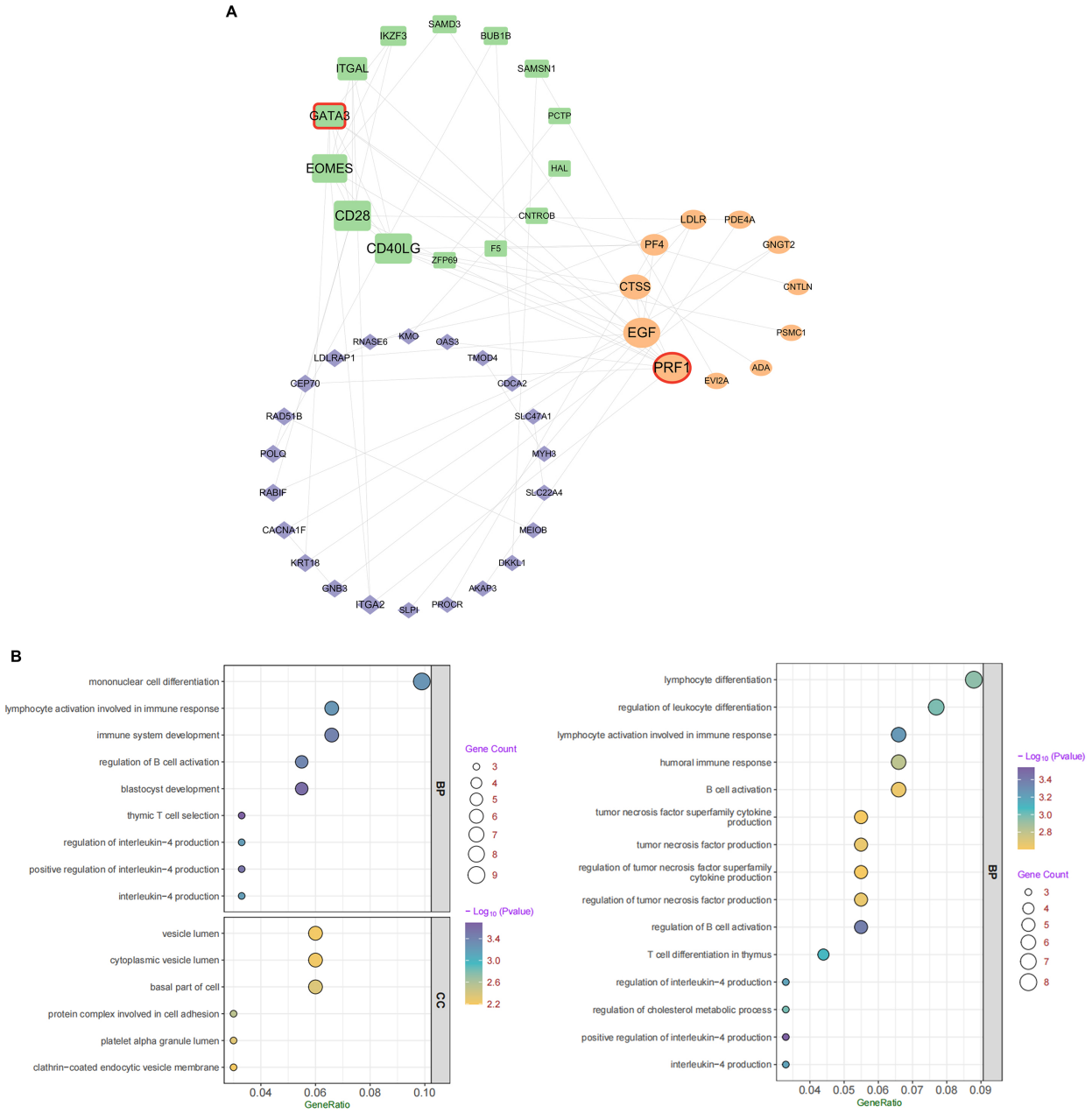

Fig. 3. Protein interaction and enrichment analysis. (A) Protein-protein interaction network of rTMS-related DEGs in SCI-NP. (B) GO enrichment of related genes to rTMS DEGs in SCI-NP. BP, Biological Process; CC, cellular component; GO, Gene Ontology.

says in spinal neurons. This transcriptional control mechanistically explained the rTMS-mediated suppression of PRF1, downregulation of pro-inflammatory cytokines (IL-1β, IL-6, TNF-α), and mitigation of pain hypersensitivity after rTMS treatment. Importantly, GATA3 overexpression abolished rTMS-mediated benefits, confirming the axis's necessity in pain pathogenesis. Notably, similar to the bilateral postural reflexes mediated by brainstem reticulospinal projections [24], rTMS may also modulate contralateral pain via descending bilateral inhibitory pathways.

Our multi-dataset analysis revealed that NP involves coordinated dysregulation of metabolic and immune pathways. The 34 coDEGs identified from GSE126611 (NP) and GSE226238 (SCI) datasets include prominent bio-enzyme coding genes (e.g., PDE4A, ADA, CTSS) alongside cytokines, receptors, and mitochondrial regulators. This molecular signature aligns with established roles of immunometabolic reprogramming in chronic NP pathogenesis [5]. Critically, hippocampal transcriptomics (GSE230149) demonstrated that rTMS induces more pronounced gene expression changes in the hippocampus than the parietal cortex. Recent studies demonstrate that spinal cord injury remotely impairs hippocampal neurogenesis via extracellular vesicle-mediated signaling. Diffu-

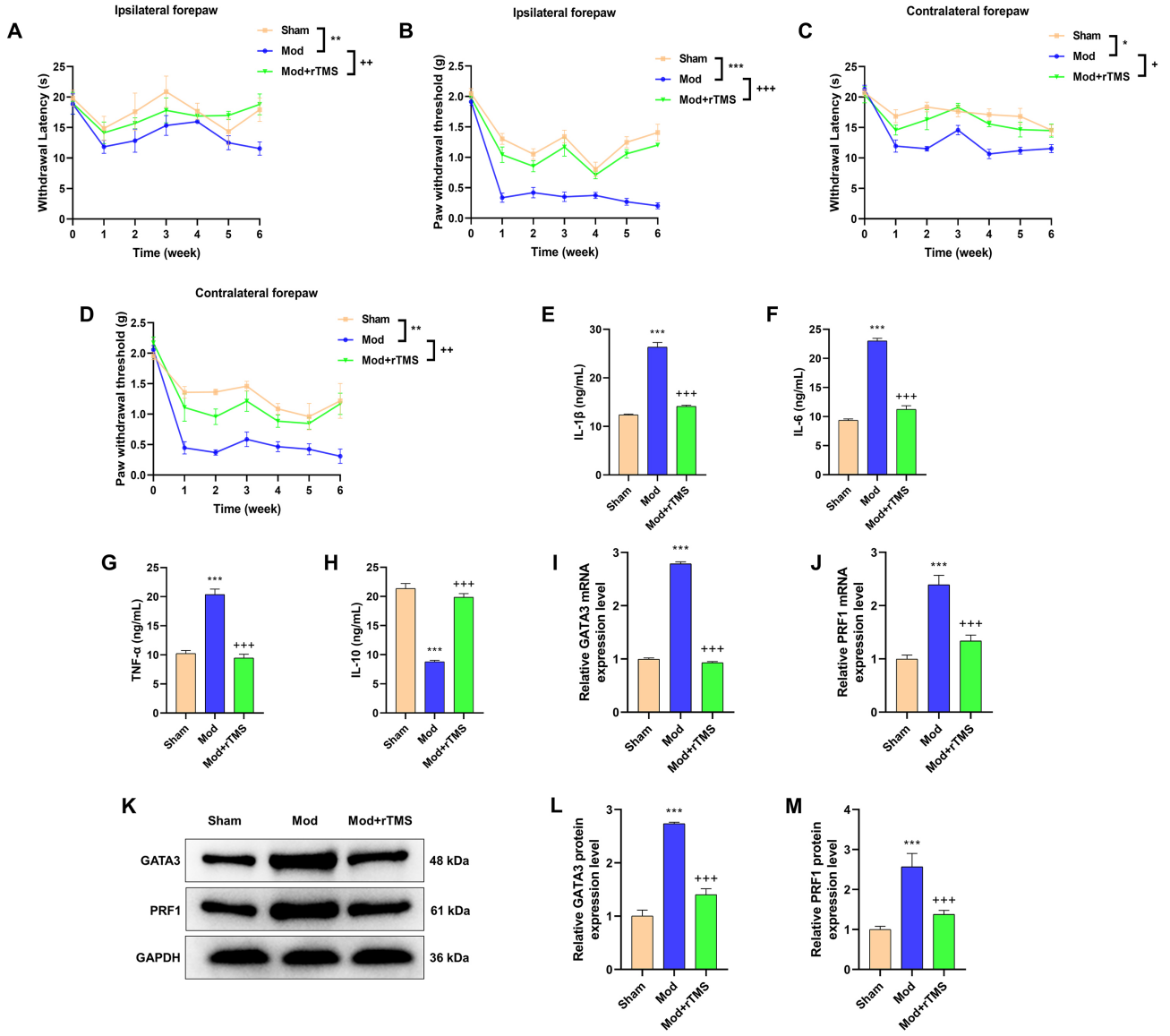

Fig. 4. rTMS alleviates SCI-NP symptoms and neuroinflammation. (A) Behavioral tests: Hargreaves (thermal hyperalgesia) in ipsilatera forepaws of the rat. (B) Behavioral tests: Von Frey (mechanical allodynia) in ipsilatera forepaws of the rat. (C) Behavioral tests: Hargreaves (thermal hyperalgesia) in contralateral forepaws of the rat. (D) Behavioral tests: Von Frey (mechanical allodynia) in contralateral forepaws of the rat. (E) The secretion level of cytokine IL-1β in spinal cord was detected by ELISA. (F) The secretion level of cytokine IL-6 in spinal cord was detected by ELISA. (G) The secretion level of cytokine TNF-α in spinal cord was detected by ELISA. (H) The secretion level of cytokine IL-10 in spinal cord was detected by ELISA. (I) The level of *GATA3* mRNA in spinal cord tissue was detected by qPCR. (J) The level of *PRF1* mRNA in spinal cord tissue was detected by qPCR. (K) The levels of GATA3 and PRF1 protein in spinal cord tissue was detected by Western blotting. (L) Western blotting analysis of relative GATA3 protein expression level. (M) Western blotting analysis of relative PRF1 protein expression level. Data: Mean ± SD, statistical significance was determined by one-way analysis of variance (ANOVA) or two-way ANOVA (A–D) followed by Tukey's post hoc test (n = 3 independent experiments); $^{*}p < 0.05$, $^{**}p < 0.01$, $^{***}p < 0.001$ vs Sham group, $^{+}p < 0.05$, $^{++}p < 0.01$, $^{+++}p < 0.001$ vs Mod group. ELISA, enzyme-linked immunosorbent assay; IL, interleukin; TNF-α, tumor necrosis factor-alpha; GATA3, GATA-binding protein 3; PRF1, Perforin 1.

sion MRI tractography has identified polysynaptic pathways linking the hippocampus to the spinal cord via brainstem nuclei [25,26]. This spatial selectivity corroborates prior evidence linking rTMS to hippocampal neuroplasticity through BDNF-mediated mechanisms [27,28].

Notably, cross-dataset mapping of rTMS-responsive DEGs onto SCI/NP cohorts revealed immune-specific convergence: key genes were exclusively enriched in immune cell signaling and response pathways (e.g., IL-4/IL-10 regulation), while bypassing hypothalamic–pituitary–adrenal

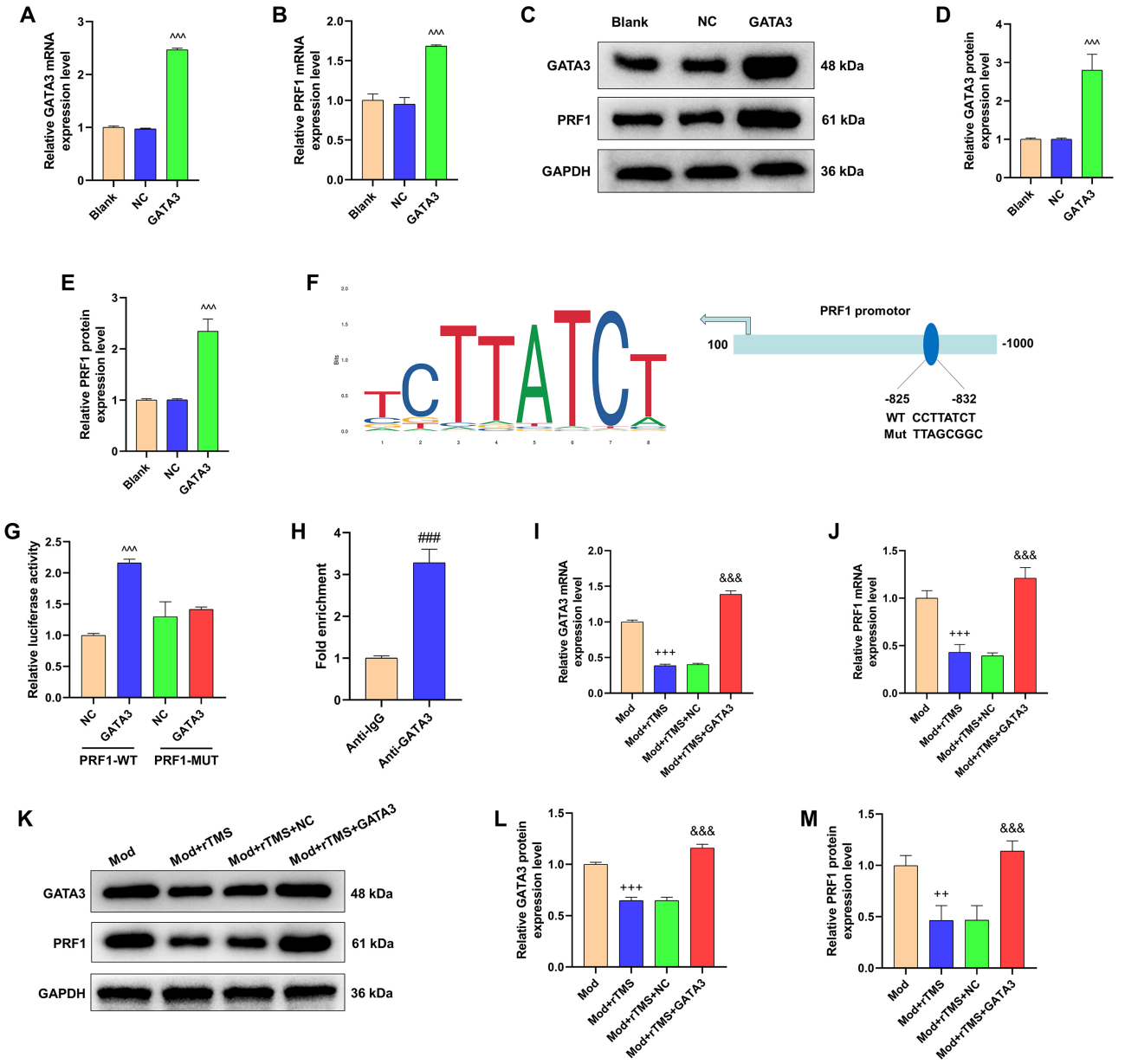

Fig. 5. GATA3 transcriptionally regulates PRF1. (A) Efficiency of GATA3 overexpression (oe-GATA3) verified by qPCR in CP-R144 neurons. (B) Effect of oe-GATA3 on *PRF1* mRNA levels by qPCR in CP-R144 neurons. (C) Efficiency of oe-GATA3 and expression level of PRF1 in CP-R144 neurons detected by Western blotting. (D) Western blotting analysis of relative GATA3 protein expression level. (E) Western blotting analysis of relative PRF1 protein expression level. (F) JASPAR prediction of GATA3 binding motif in PRF1 promoter. (G) Dual-luciferase assay: PRF1 promoter activity under oe-GATA3. (H) ChIP confirming GATA3 binding to PRF1 promoter. (I) The level of *GATA3* mRNA in SCI-NP rats treated with rTMS and GATA3 was detected by qPCR. (J) The level of *PRF1* mRNA in SCI-NP rats treated with rTMS and GATA3 was detected by qPCR. (K) The levels of GATA3 and PRF1 protein in SCI-NP rats treated with rTMS and GATA3 was detected by Western blotting. (L) Western blotting analysis of relative GATA3 protein expression level. (M) Western blotting analysis of relative PRF1 protein expression level. Data: Mean ± SD, statistical significance was determined by one-way analysis of variance (ANOVA) or Student's *t*-test (H) followed by Tukey's post hoc test (n = 3 independent experiments); $^{\wedge\wedge\wedge}p < 0.001$ *vs* NC; $^{\#\#\#}p < 0.001$ *vs* Anti-IgG; $^{++}p < 0.01$, $^{+++}p < 0.001$ *vs* Mod group; $^{\&\&\&}p < 0.001$ *vs* Mod + rTMS + NC group. ChIP, Chromatin immunoprecipitation.

(HPA) axis or apoptosis mechanisms typically associated with rTMS effects in depression [29]. This immunological focus is consistent with recent clinical observations where 8-week rTMS alleviated cognitive deficits in NP through immunomodulation, distinct from its antidepressant effects [30]. The absence of HPA-axis enrichment underscores a

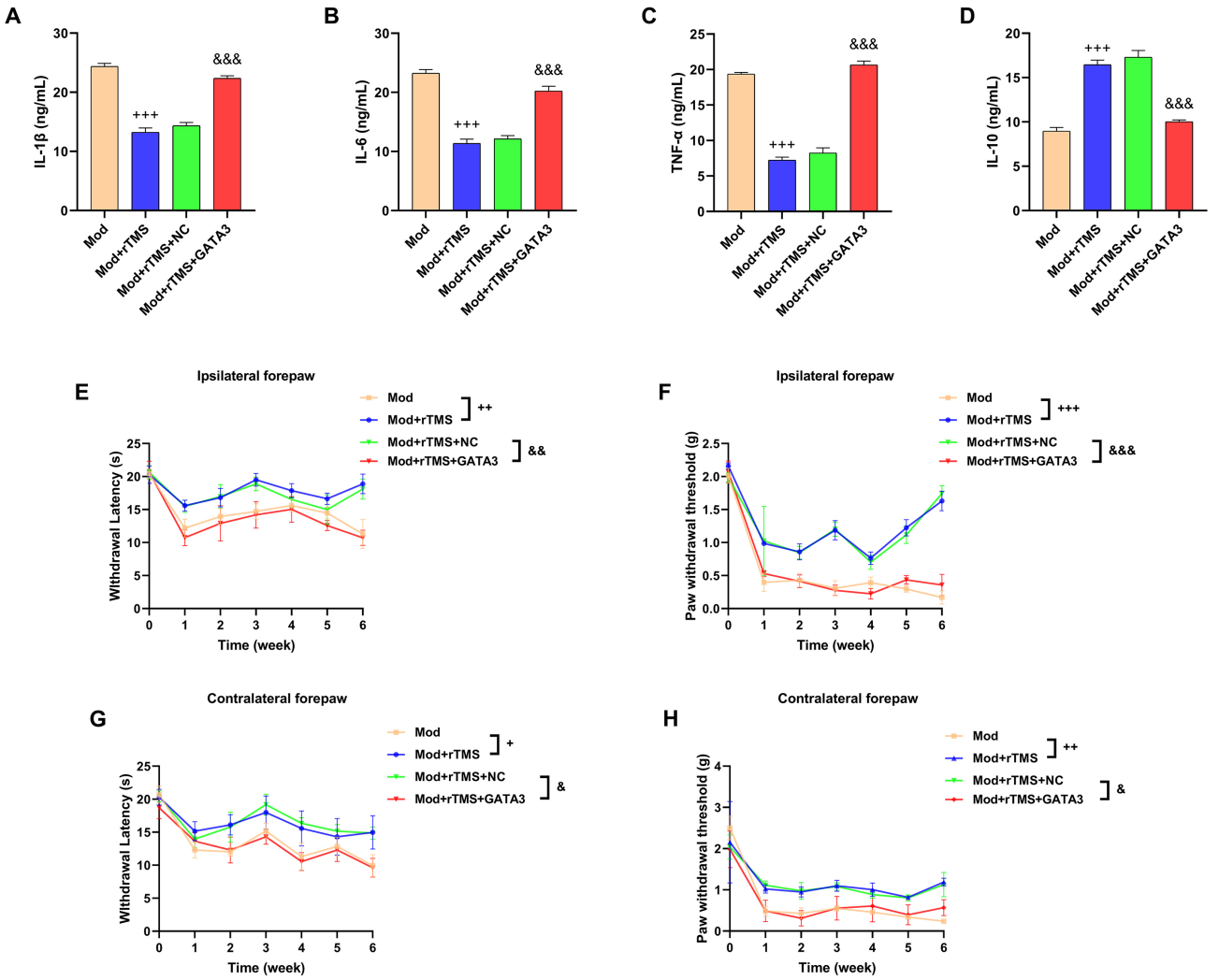

Fig. 6. GATA3 overexpression reverses rTMS-mediated protection. (A) The secretion level of cytokine IL-1β in SCI-NP rats treated with rTMS and GATA3 was detected by ELISA. (B) The secretion level of cytokine IL-6 in SCI-NP rats treated with rTMS and GATA3 was detected by ELISA. (C) The secretion level of cytokine TNF-α in SCI-NP rats treated with rTMS and GATA3 was detected by ELISA. (D) The secretion level of cytokine IL-10 in SCI-NP rats treated with rTMS and GATA3 was detected by ELISA. (E) Behavioral tests: Hargreaves (thermal hyperalgesia) in ipsilatera forepaws in SCI-NP rats treated with rTMS and GATA3. (F) Behavioral tests: Von Frey (mechanical allodynia) in ipsilatera forepaws in SCI-NP rats treated with rTMS and GATA3. (G) Behavioral tests: Hargreaves (thermal hyperalgesia) in contralateral forepaws in SCI-NP rats treated with rTMS and GATA3. (H) Behavioral tests: Von Frey (mechanical allodynia) in contralateral forepaws in SCI-NP rats treated with rTMS and GATA3. Data: Mean ± SD, statistical significance was determined by one-way analysis of variance (ANOVA) or two-way ANOVA (E–H) followed by Tukey's post hoc test (n = 3 independent experiments); $^{+}p < 0.05$, $^{++}p < 0.01$, $^{+++}p < 0.001$ vs Mod group; $^{\&}p < 0.05$, $^{\&\&}p < 0.01$, $^{\&\&\&}p < 0.001$ vs Mod + rTMS + NC group.

unique mechanism for rTMS in SCI-NP, potentially mediated through interleukin crosstalk within hippocampal-immune circuits.

Conventional investigations into magnetic neuromodulation have predominantly emphasized direct neuroprotective processes. For example, dual-target magnetic stimulation (DTMS) has been shown to attenuate oligodendrocyte apoptosis through GAP43-mediated myelin regeneration [31], while systemic magnetic field therapy activates the PI3K/Akt axis to reduce neuronal loss [32]. In contrast, our findings fundamentally transcend the neurocentric paradigm by establishing an immunomodulatory axis through which rTMS mitigates neuroinflammation in SCI-NP. This pathway orchestrates dual cytokine reprogramming: suppression of pro-inflammatory mediators (IL-1β, IL-6, TNF-α) concurrent with potentiation of anti-inflammatory IL-10. This immunobiological cascade aligns with our prior bioinformatic evidence demonstrating enriched cytokine-cytokine receptor interactions among key gene targets.

The conserved pathophysiological function of PRF1, as a cardinal executor of $CD8^+$ T lymphocyte cytotoxicity, extends beyond peripheral immunity into neural circuits. Compelling evidence documents its dual capacity to instigate target cell lysis and propagate inflammatory cascades. For instance, in inflammatory bowel disease, PRF1 released from colonic $CD8^+$ T effectors has been shown to induce hippocampal endoplasmic reticulum stress, thereby contributing to depression through gut-brain axis dysregulation [33]. Similarly, spinal cord microenvironments exhibit exacerbated neural damage following $PRF1^+$ $CD8^+$ T cell infiltration, impeding functional recovery [34]. While direct evidence linking PRF1 to SCI-NP is limited in current literature, mutations in the PRF1 gene cause central nervous system (CNS) damage by inducing hemophagocytic lymphohistiocytosis (HLH) [35]. The coexistence of chronic hyperalgesia and multilevel neuroinflammation post-SCI suggests that immune-derived factors may perpetuate pain by sustaining neuronal sensitization and glial activation [36]. Our findings suggest that rTMS-mediated suppression of both PRF1 expression and neuroinflammatory markers (IL-1β/IL-6/TNF-α) aligns mechanistically with GATA3's transcriptional governance. This convergence indicates that dampening the GATA3-PRF1 axis may disrupt neuro-immune communication pathways common to diverse neurological disorders, but does not exclude other mechanisms. Future studies using cell-type specific knockout models and ChIP assays will be needed to establish direct regulatory relationships.

This study bridges a critical conceptual gap between neuroinflammation and neuromodulation by identifying the GATA3-PRF1 axis as a unified effector pathway for rTMS in SCI-NP. Therapeutically, rTMS leverages non-invasive neuromodulation that enables spatially confined immunosuppression—surpassing conventional pharmacological interventions limited by systemic toxicity or the blood-brain barrier. Clinical translatability is further enhanced by its established FDA-cleared safety profile for neurological disorders, protocol alignment with established rTMS regimens (6-week course), and compatibility with emerging precision technologies such as focused ultrasound neuroregulation or bioengineered neural scaffolds. These advantages position rTMS as a scalable strategy for mitigating neuroimmune cascades while avoiding risks inherent to viral vector-based gene therapies or chronic drug administration. Our study provides preliminary evidence that rTMS may alleviate SCI-NP by suppressing the GATA3-PRF1 axis. However, the specific cellular sources of GATA3 and PRF1 are unknown. Future studies using spatial transcriptomics or multiplex immunofluorescence will be required to validate their cell-type specificity.

This study has several limitations. First, despite these advances, the cellular specificity of GATA3 within the spinal immune niche requires further clarification. Single-cell chromatin accessibility profiling (e.g., scATAC-seq) will be essential to determine whether GATA3 operates predominantly in $CD8^+$ T lymphocytes, NK cells, or infiltrating macrophages—a distinction vital for target refinement. Second, evolutionary conservation analyses raise the possibility of divergence in GATA3-PRF1 interactions across vertebrates, underscoring the need for cross-species validation to assess mechanistic universality. Third, future therapeutic strategies may benefit from combinatorial approaches that integrate dynamically responsive biomaterials (e.g., glucan hydrogels patterned with neuronal guidance cues) or JAK2 pathway inhibitors (approved by the FDA for autoimmune diseases) to amplify neuroimmune restoration, particularly in refractory cases where monotherapy proves insufficient. Such multimodal synergy could unlock regenerative capacities beyond immunomodulation alone. Finally, although this study establishes a regulatory link between GATA3 and PRF1, the downstream mechanisms of PRF1 in the context of SCI remain to be fully elucidated. Conditional knockout models or single-cell cytokine profiling will be required to assess whether PRF1 directly modulates immune responses in this setting.

Conclusion

In summary, this study demonstrates that rTMS alleviates SCI-NP by targeting the GATA3-PRF1 neuroimmune axis. Specifically, rTMS reduced GATA3-mediated transcriptional activation of PRF1, a key cytotoxic effector molecule, leading to reduced neuroinflammation and subsequent pain hypersensitivity. However, given the pleiotropic nature of rTMS, future studies should investigate how this pathway interacts with other known rTMS targets to produce the overall therapeutic effect.

Availability of Data and Materials

The analyzed data sets generated during the study are available from the corresponding author on reasonable request.

Author Contributions

QZ and YZ designed the research study; YO performed the research; YW, WZ and QL collected and analyzed the data; WZ has been involved in drafting the manuscript. All authors have been involved in revising the manuscript critically for important intellectual content. All authors give final approval of the version to be published. All authors have participated sufficiently in the work to take public responsibility for appropriate portions of the content and agreed to be accountable for all aspects of the work in ensuring that questions related to its accuracy or integrity.

Ethics Approval and Consent to Participate

All animal experiments received prior approval from Laboratory Animal Welfare and Ethics Committee of Institutional Animal Care and Use Committee, Zhejiang Center of Laboratory Animals (Approval No. ZJCLA-IACUC-20010727), and strictly adhered to the guidelines of the China Council on Animal Care and Use Health.

Acknowledgment

Not applicable.

Funding

This work was supported by Zhejiang Province Medical and Health Science and Technology Project [grant numbers 2021KY044] and Zhejiang Province Medical and Health Science and Technology Project [grant numbers 2022KY604].

Conflict of Interest

The authors declare no conflict of interest.

References

[1] Finnerup NB, Haroutounian S, Kamerman P, Baron R, Bennett DLH, Bouhassira D, *et al*. Neuropathic pain: an updated grading system for research and clinical practice. Pain. 2016; 157: 1599–1606. https://doi.org/10.1097/j.pain.0000000000000492.

[2] Macone A, Otis JAD. Neuropathic Pain. Seminars in Neurology. 2018; 38: 644–653. https://doi.org/10.1055/s-0038-1673679.

[3] Burke D, Fullen BM, Stokes D, Lennon O. Neuropathic pain prevalence following spinal cord injury: A systematic review and meta-analysis. European Journal of Pain (London, England). 2017; 21: 29–44. https://doi.org/10.1002/ejp.905.

[4] Attal N, Bouhassira D. Chapter 47 Pain in syringomyelia/bulbia. Handbook of Clinical Neurology. 2006; 81: 705–713. https://doi.org/10.1016/S0072-9752(06)80051-5.

[5] Attal N. Spinal cord injury pain. Revue Neurologique. 2021; 177: 606–612. https://doi.org/10.1016/j.neurol.2020.07.003.

[6] Knotkova H, Hamani C, Sivanesan E, Le Beuffe MFE, Moon JY, Cohen SP, *et al*. Neuromodulation for chronic pain. Lancet (London, England). 2021; 397: 2111–2124. https://doi.org/10.1016/S0140-6736(21)00794-7.

[7] Ferraro MC, Gibson W, Rice ASC, Vase L, Coyle D, O'Connell NE. Spinal cord stimulation for chronic pain. The Lancet. Neurology. 2022; 21: 405. https://doi.org/10.1016/S1474-4422(22)00096-5.

[8] Pan LJ, Zhu HQ, Zhang XA, Wang XQ. The mechanism and effect of repetitive transcranial magnetic stimulation for post-stroke pain. Frontiers in Molecular Neuroscience. 2023; 15: 1091402. https://doi.org/10.3389/fnmol.2022.1091402.

[9] Phillips AL, Burr RL, Dunner DL. Repetitive Transcranial Magnetic Stimulation in the Treatment of Bipolar Depression: Experience From a Clinical Setting. Journal of Psychiatric Practice. 2020; 26: 37–45. https://doi.org/10.1097/PRA.0000000000000447.

[10] Borodulina IV. Repetitive transcranial magnetic stimulation in the treatment Parkinson's disease patients. Brain Stimulation: Basic, Translational, and Clinical Research in Neuromodulation. 2019; 12: e129–e130. https://doi.org/10.1016/j.brs.2019.03.031.

[11] Hsu JH, Daskalakis ZJ, Blumberger DM. An Update on Repetitive Transcranial Magnetic Stimulation for the Treatment of Co-morbid Pain and Depressive Symptoms. Current Pain and Headache Reports. 2018; 22: 51. https://doi.org/10.1007/s11916-018-0703-7.

[12] Bacha R, Pedersen S, Ismail R, Alwisi N, Al-Mansoori L. GATA3: Orchestrating cellular fate through differentiation and proliferation. Biochimica et Biophysica Acta. Molecular Cell Research. 2025; 1872: 119893. https://doi.org/10.1016/j.bbamcr.2024.119893.

[13] Ho IC, Tai TS, Pai SY. GATA3 and the T-cell lineage: essential functions before and after T-helper-2-cell differentiation. Nature Reviews. Immunology. 2009; 9: 125–135. https://doi.org/10.1038/nri2476.

[14] Zhuang J, Chen P, Wu Y, Luo Q, Wang Q, Chen S, *et al*. *Brca1* Is Regulated by the Transcription Factor *Gata3*, and Its Silencing Promotes Neural Differentiation in Retinal Neurons. International Journal of Molecular Sciences. 2022; 23: 13860. https://doi.org/10.3390/ijms232213860.

[15] Zheng Y, Sun Y, Yang Y, Zhang S, Xu T, Xin W, *et al*. GATA3-dependent epigenetic upregulation of CCL21 is involved in the development of neuropathic pain induced by bortezomib. Molecular Pain. 2019; 15: 1744806919863292. https://doi.org/10.1177/1744806919863292.

[16] Cheng J, Wang D, Geng M, Zheng Y, Cao Y, Liu S, *et al*. Transcription factor networks drive perforin activity in the antibacterial immune response of tilapia. Fish & Shellfish Immunology. 2024; 154: 109975. https://doi.org/10.1016/j.fsi.2024.109975.

[17] Willenbring RC, Johnson AJ. Finding a Balance between Protection and Pathology: The Dual Role of Perforin in Human Disease. International Journal of Molecular Sciences. 2017; 18: 1608. https://doi.org/10.3390/ijms18081608.

[18] Robinson MD, McCarthy DJ, Smyth GK. edgeR: a Bioconductor package for differential expression analysis of digital gene expression data. Bioinformatics (Oxford, England). 2010; 26: 139–140. https://doi.org/10.1093/bioinformatics/btp616.

[19] Ritchie ME, Phipson B, Wu D, Hu Y, Law CW, Shi W, *et al*. limma powers differential expression analyses for RNA-sequencing and microarray studies. Nucleic Acids Research. 2015; 43: e47. https://doi.org/10.1093/nar/gkv007.

[20] Wu T, Hu E, Xu S, Chen M, Guo P, Dai Z, *et al*. clusterProfiler 4.0: A universal enrichment tool for interpreting omics data. Innovation (Cambridge (Mass.)). 2021; 2: 100141. https://doi.org/10.1016/j.xinn.2021.100141.

[21] Brown EV, Falnikar A, Heinsinger N, Cheng L, Andrews CE, DeMarco M, *et al*. Cervical spinal cord injury-induced neuropathic pain in male mice is associated with a persistent pro-inflammatory macrophage/microglial response in the superficial dorsal horn. Experimental Neurology. 2021; 343: 113757. https://doi.org/10.1016/j.expneurol.2021.113757.

[22] Zhang L, Xiao Z, Su Z, Wang X, Tian H, Su M. Repetitive transcranial magnetic stimulation promotes motor function recovery in mice after spinal cord injury via regulation of the Cx43-autophagy loop. Journal of Orthopaedic Surgery and Research. 2024; 19: 387. https://doi.org/10.1186/s13018-024-04879-6.

[23] Xu T, Wang J, Wu Y, Wu JY, Lu WC, Liu M, *et al*. Ac4C Enhances the Translation Efficiency of Vegfa mRNA and Mediates Central Sensitization in Spinal Dorsal Horn in Neuropathic Pain. Advanced Science (Weinheim, Baden-Wurttemberg, Germany). 2023; 10: e2303113. https://doi.org/10.1002/advs.202303113.

[24] Todd NPM, Govender S, Lemieux L, Colebatch JG. Source analyses of axial and vestibular evoked potentials associated with brainstem-spinal reflexes show cerebellar and cortical contribu-

tions. Neuroscience Letters. 2021; 757: 135960. https://doi.org/10.1016/j.neulet.2021.135960.

[25] Soltani Zangbar H, Ghadiri T, Vafaee MS, Ebrahimi Kalan A, Karimipour M, Fallahi S, *et al*. A potential entanglement between the spinal cord and hippocampus: Theta rhythm correlates with neurogenesis deficiency following spinal cord injury in male rats. Journal of Neuroscience Research. 2020; 98: 2451–2467. https://doi.org/10.1002/jnr.24719.

[26] Arrigo A, Mormina E, Calamuneri A, Gaeta M, Marino S, Milardi D, *et al*. Amygdalar and hippocampal connections with brainstem and spinal cord: A diffusion MRI study in human brain. Neuroscience. 2017; 343: 346–354. https://doi.org/10.1016/j.neuroscience.2016.12.016.

[27] Ahmed Z, Wieraszko A. Modulation of learning and hippocampal, neuronal plasticity by repetitive transcranial magnetic stimulation (rTMS). Bioelectromagnetics. 2006; 27: 288–294. https://doi.org/10.1002/bem.20211.

[28] Yulug B, Hanoglu L, Khanmammadov E, Duz OA, Polat B, Hanoglu T, *et al*. Beyond The Therapeutic Effect of rTMS in Alzheimer's Disease: A Possible Neuroprotective Role of Hippocampal BDNF?: A Minireview. Mini Reviews in Medicinal Chemistry. 2018; 18: 1479–1485. https://doi.org/10.2174/1389557517666170927162537.

[29] Zhao L, Ren H, Gu S, Li X, Jiang C, Li J, *et al*. rTMS ameliorated depressive-like behaviors by restoring HPA axis balance and prohibiting hippocampal neuron apoptosis in a rat model of depression. Psychiatry Research. 2018; 269: 126–133. https://doi.org/10.1016/j.psychres.2018.08.017.

[30] Boylu ME, Turan Ş, Güler EM, Boylu FB, Kılıç Ö, Koçyiğit A, *et al*. Changes in neuroactive steroids, neurotrophins and immunological biomarkers after monotherapy 8-week rTMS treatment and their relationship with neurocognitive functions in depression. European Archives of Psychiatry and Clinical Neuroscience. 2024; 274: 849–865. https://doi.org/10.1007/s00406-023-01704-9.

[31] Huang M, Di J, He L, Li N, Tian Z, Xiao L, *et al*. Double-target magnetic stimulation attenuates oligodendrocyte apoptosis and oxidative stress impairment after spinal cord injury via GAP43. The Spine Journal: Official Journal of the North American Spine Society. 2025; 25: 820–842. https://doi.org/10.1016/j.spinee.2024.12.025.

[32] Liu Z, Lin Z, Liu X, Xie X, Tan C. Application and progress of magnetic field therapy for spinal cord injury. Journal of Neurorestoratology. 2025; 13: 100205. https://doi.org/10.1016/j.jnrt.2025.100205.

[33] Huang S, Pan L, Pang S, Guo H, Li M, Tian Y, *et al*. Perforin Generated by $CD8^+$ T Cells Exacerbates Inflammatory Bowel Disease-Induced Depression by Promoting CXCL9 Production in Intestinal Epithelial Cells. Gastroenterology. 2025; 169: 294–307. https://doi.org/10.1053/j.gastro.2025.02.036.

[34] Liu Z, Zhang H, Xia H, Wang B, Zhang R, Zeng Q, *et al*. CD8 T cell-derived perforin aggravates secondary spinal cord injury through destroying the blood-spinal cord barrier. Biochemical and Biophysical Research Communications. 2019; 512: 367–372. https://doi.org/10.1016/j.bbrc.2019.03.002.

[35] You Y, Wu W, Li B. Familial hemophagocytic phohistiocytosis induced by PRF1 mutation with neurologic manifestations as the initial clinical presentations: A case report. Medicine. 2023; 102: e34198. https://doi.org/10.1097/MD.0000000000034198.

[36] Wang L, Gunduz MA, Semeano AT, Yılmaz EC, Alanazi FAH, Imir OB, *et al*. Coexistence of chronic hyperalgesia and multilevel neuroinflammatory responses after experimental SCI: a systematic approach to profiling neuropathic pain. Journal of Neuroinflammation. 2022; 19: 264. https://doi.org/10.1186/s12974-022-02628-2.